

Springer Topics in Signal Processing

Boaz Rafaely

# Fundamentals of Spherical Array Processing

# **Springer Topics in Signal Processing**

**Volume 8**

## **Series editors**

Jacob Benesty, Montreal, Canada

Walter Kellermann, Erlangen, Germany

More information about this series at <http://www.springer.com/series/8109>

Boaz Rafaely

# Fundamentals of Spherical Array Processing



Springer

Boaz Rafaely  
Department of Electrical and Computer  
Engineering  
Ben-Gurion University of the Negev  
Beer-Sheva  
Israel

ISSN 1866-2609                    ISSN 1866-2617 (electronic)  
Springer Topics in Signal Processing  
ISBN 978-3-662-45663-7        ISBN 978-3-662-45664-4 (eBook)  
DOI 10.1007/978-3-662-45664-4

Library of Congress Control Number: 2014955795

Springer Heidelberg New York Dordrecht London  
© Springer-Verlag Berlin Heidelberg 2015

This work is subject to copyright. All rights are reserved by the Publisher, whether the whole or part of the material is concerned, specifically the rights of translation, reprinting, reuse of illustrations, recitation, broadcasting, reproduction on microfilms or in any other physical way, and transmission or information storage and retrieval, electronic adaptation, computer software, or by similar or dissimilar methodology now known or hereafter developed.

The use of general descriptive names, registered names, trademarks, service marks, etc. in this publication does not imply, even in the absence of a specific statement, that such names are exempt from the relevant protective laws and regulations and therefore free for general use.

The publisher, the authors and the editors are safe to assume that the advice and information in this book are believed to be true and accurate at the date of publication. Neither the publisher nor the authors or the editors give a warranty, express or implied, with respect to the material contained herein or for any errors or omissions that may have been made.

Printed on acid-free paper

Springer-Verlag GmbH Berlin Heidelberg is part of Springer Science+Business Media  
([www.springer.com](http://www.springer.com))

*To my parents, Nitzan and Rivka Rafaely*

# Preface

Microphone arrays and associated array processing techniques have been developed for a wide range of applications over the past few decades. These applications include speech communication, music recording, room acoustics analysis, noise control and acoustic holography, defense and security, entertainment, and many more. In the cases of speech in rooms and music in concert halls, the sound tends to travel throughout the entire enclosed space, producing a three-dimensional sound field. Microphone arrays that effectively measure and process three-dimensional sound fields typically require the positioning of microphones within a volume in three-dimensional space. Planar arrays, mounted on an enclosure wall, have been studied for several decades, while more recently, spherical arrays, in which microphones are mounted around a rigid sphere, for example, have been developed. These offer several advantages over classical linear, rectangular, or circular arrays:

- (i) The sphere, having complete rotational symmetry, facilitates spatial filtering, or beamforming, that can be designed to effectively enhance or attenuate sources in any direction.
- (ii) Array processing and performance analysis can be formulated in the spherical harmonics domain, which is the Fourier domain for the sphere. This domain facilitates efficient algorithms and extensive acoustic modeling of both the array and the surrounding sound field.
- (iii) Beamforming can be efficiently implemented by decoupling beam pattern design from beam pattern steering, therefore providing simplicity and flexibility in array realization.

These advantages have motivated an increasing number of researchers in recent years to develop spherical microphone array systems, to study spherical array configurations, to develop algorithms for spherical arrays, and to apply these arrays in a wide range of applications. This growing activity has provided the author with the motivation and inspiration to write this book, with the aim of presenting the fundamentals of spherical array processing in a tutorial manner suitable for researchers, graduate students, and engineers interested in this topic.

The first two chapters provide the reader with the necessary mathematical and physical background, including an introduction to the spherical Fourier transform and to the formulation of plane-wave sound fields in the spherical harmonics domain. The third chapter covers the theory of spatial sampling, which becomes useful when selecting the positions of microphones to sample sound pressure functions in space. The next chapter presents various spherical array configurations, including the popular configuration based on a rigid sphere. The fifth chapter introduces the concept of beamforming and its basic equations, including popular design methods such as delay-and-sum and regular beamforming. The following chapter presents methods for the optimal design of beam patterns, formulated to achieve various objectives, such as maximum robustness, maximum directivity, or minimum side-lobe level. The final chapter develops more advanced array processing algorithms, such as the minimum variance distortionless response (MVDR) algorithm. These algorithms aim to enhance a desired signal while attenuating undesired noise components in the sound field by exploring their unique formulation in the spherical harmonics domain.

My own interest in spherical array processing began during a six-month visit to the sensory communication group at MIT in 2002, working with Julie Greenberg and greatly enjoying the stimulating vibe of Boston. I would like to thank Julie for providing this opportunity, for the hospitality, and for the helpful discussions. During my visit to Boston I was exposed to the inspiring publications on spherical arrays by Jens Meyer and Gary Elko. Their pioneering work planted the seeds that later flourished to an extensive research effort at my lab, the acoustics laboratory, Ben-Gurion University of the Negev. The research at the acoustics laboratory was pursued by an invaluable cooperation with a great number of research students, postdoctoral researchers, and visitors. The relaxed atmosphere at the lab, the great teamwork, and the endless discussions were the fuel that kept the writing of this book viable. I would like to express great thanks to the acoustics laboratory researchers: Dr. Jonathan Sheaffer, Dr. Jonathan Rathsam, Dr. Noam Shabtai, Dr. Dror Lederman, Dr. Yotam Peled, Dr. Etan Fisher, Vladimir Tournabin, Hai Morgenstern, David Alon, Koby Alhaiany, Mickey Jeffet, Elad Cohen, Dima Lvov, Or Nadiri, Shahar Villeval, Tal Szpruch, Nejem Hulihel, Ilan Ben-Hagai, Tomer Peleg, Amir Avni, Morag Agmon, Maor Klieder, Dima Haykin, Itai Peer, and Ilya Balmages. Also, special thanks to Dr. Franz Zotter for the helpful comments on a draft version of the manuscript made during a visit to the lab. Thanks also to Debbie Kedar for the prompt and professional editing and proofreading of this book. Finally, thanks to my family, Vered, Asaf, Yonathan, and Tal, for providing love therapy that time and again pulled me out of the writing stumbles and falls.

Beer-Sheva, December 2014

Boaz Rafaely

# Contents

<b>1 Mathematical Background . . . . .</b>	1
1.1 Functions on the Sphere . . . . .	1
1.2 Spherical Harmonics . . . . .	4
1.3 Exponential and Legendre Functions . . . . .	12
1.4 Spherical Fourier Transform . . . . .	16
1.5 Some Useful Functions . . . . .	21
1.6 Rotation of Functions . . . . .	24
1.7 Spherical Convolution and Correlation . . . . .	28
<b>2 Acoustical Background . . . . .</b>	31
2.1 The Acoustic Wave Equation . . . . .	31
2.2 Spherical Bessel and Hankel Functions . . . . .	34
2.3 A Single Plane Wave . . . . .	38
2.4 Plane-Wave Composition . . . . .	42
2.5 Point Sources . . . . .	45
2.6 Sound Pressure Around a Rigid Sphere . . . . .	47
2.7 Translations of Fields . . . . .	52
<b>3 Sampling the Sphere . . . . .</b>	57
3.1 Sampling Order-Limited Functions . . . . .	57
3.2 Equal-Angle Sampling . . . . .	59
3.3 Gaussian Sampling . . . . .	64
3.4 Uniform and Nearly-Uniform Sampling . . . . .	65
3.5 Numerical Computation of Sampling Weights . . . . .	68
3.6 The Discrete Spherical Fourier Transform . . . . .	71
3.7 Spatial Aliasing . . . . .	73
<b>4 Spherical Array Configurations . . . . .</b>	79
4.1 Single Open Sphere . . . . .	80
4.2 Rigid Sphere . . . . .	83
4.3 Open Sphere with Cardioid Microphones . . . . .	85

4.4	Dual-Radius Open Sphere . . . . .	87
4.5	Robustness to Errors and Numerical Array Design . . . . .	90
4.6	Design Examples with Robustness Analysis . . . . .	93
4.7	Spherical Shell Configuration . . . . .	95
4.8	Other Configurations . . . . .	98
<b>5</b>	<b>Spherical Array Beamforming . . . . .</b>	101
5.1	Beamforming Equations . . . . .	101
5.2	Axis-Symmetric Beamforming . . . . .	106
5.3	Directivity Index . . . . .	109
5.4	White Noise Gain . . . . .	111
5.5	Simple Axis-Symmetric Beamformers . . . . .	114
5.6	Beamforming Example . . . . .	116
5.7	Steering Non Axis-Symmetric Beam Patterns . . . . .	121
<b>6</b>	<b>Optimal Beam Pattern Design . . . . .</b>	125
6.1	Maximum Directivity Beamformer . . . . .	125
6.2	Maximum WNG Beamformer . . . . .	130
6.3	Example: Directivity Versus WNG . . . . .	133
6.4	Mixed Objectives . . . . .	135
6.5	Maximum Front-Back Ratio . . . . .	139
6.6	Dolph-Chebyshev Beam Pattern . . . . .	142
6.7	Multiple-Objective Design . . . . .	147
<b>7</b>	<b>Beamforming with Noise Minimization . . . . .</b>	155
7.1	Beamforming Equations Including Noise . . . . .	155
7.2	Minimum Variance Distortionless Response . . . . .	160
7.3	Example: MVDR with Sensor Noise and Disturbance . . . . .	164
7.4	Example: MVDR with Correlated Disturbance . . . . .	166
7.5	Linearly Constrained Minimum Variance . . . . .	169
7.6	Example: LCMV with Beam Pattern Amplitude Constraints . . . . .	172
7.7	LCMV with Derivative Constraints . . . . .	176
7.8	Example: Robust LCMV with Derivative Constraints . . . . .	178
<b>Errata to: Fundamentals of Spherical Array Processing . . . . .</b>	E1	
<b>Glossary . . . . .</b>	183	
<b>References . . . . .</b>	187	
<b>Index . . . . .</b>	191	

# Chapter 1

## Mathematical Background

**Abstract** This chapter provides the mathematical background necessary for studying spherical array processing. Spherical arrays typically sample functions on a sphere (e.g. sound pressure); therefore, this chapter begins by presenting the spherical coordinate system as well as some examples of functions on the sphere. Spherical harmonics are a central theme of this book as they form a basis for representing functions on the sphere. Therefore, spherical harmonics are first defined and illustrated, and then an introduction to the spherical Fourier transform and a description of functions on the sphere in Hilbert space follows. The chapter concludes with a presentation of the topics of rotation, convolution, and correlation defined for functions on the sphere.

### 1.1 Functions on the Sphere

Consider the standard Cartesian coordinate system with coordinates

$$\mathbf{x} \equiv (x, y, z) \in \mathbb{R}^3, \quad (1.1)$$

where  $\mathbb{R}^3$  is the three-dimensional space of real numbers and  $\mathbf{x}$  represents a vector in geometric notation. A spherical surface of unit radius, denoted by  $S^2$ , can be defined in the Cartesian coordinate system as

$$S^2 = \{\mathbf{x} \in \mathbb{R}^3 : \|\mathbf{x}\| = 1\}, \quad (1.2)$$

which represents all positions having unit distance from the origin, with  $\|\cdot\|$  denoting the Euclidean norm. Positions on  $S^2$  can be denoted by elevation and azimuth angles,  $\theta$  and  $\phi$ , which define the spherical coordinates, together with the radial distance (or radius),  $r$ :

$$\mathbf{r} \equiv (r, \theta, \phi). \quad (1.3)$$

---

The erratum of this chapter can be found under DOI [10.1007/978-3-662-45664-4\\_8](https://doi.org/10.1007/978-3-662-45664-4_8)

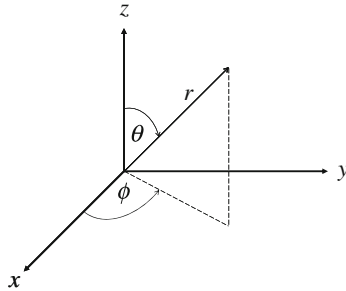


**Fig. 1.1** Spherical coordinate system defined relative to the Cartesian coordinate system

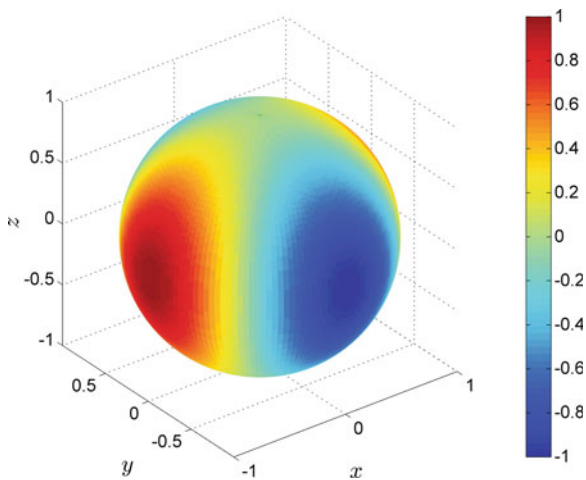


**Fig. 1.2** Plot of function  $f(\theta, \phi) = \sin^2 \theta \cos(2\phi)$  over the surface of a *unit sphere*

The azimuth angle  $\phi$  is measured from the  $x$ -axis towards the  $y$ -axis, while the elevation angle  $\theta$  is measured downwards from the  $z$ -axis, as illustrated in Fig. 1.1.

A position  $\mathbf{r} = (r, \theta, \phi)$  represented in spherical coordinates can be related to the same position represented in Cartesian coordinates  $\mathbf{x} = (x, y, z)$  using

$$\begin{aligned} x &= r \sin \theta \cos \phi \\ y &= r \sin \theta \sin \phi \\ z &= r \cos \theta. \end{aligned} \tag{1.4}$$

Spherical functions, or functions defined over the unit sphere, are central to this book. An example of a function over the sphere is

$$f(\theta, \phi) = \sin^2 \theta \cos(2\phi). \quad (1.5)$$

The function can be presented graphically in various ways: as a color map on the surface of a unit sphere, as in Fig. 1.2, as a color contour map on a  $\theta\phi$  plane mapping the surface of a unit sphere, as in Fig. 1.3, and with magnitude denoted by the distance from the origin (balloon plot), as in Fig. 1.4. In the latter plot, cyan (green-blue) shades represent positive values, while magenta (purple-red) shades represent negative values. All three figures show one maximum and two zeros over  $\theta$ , due to the  $\sin^2 \theta$  term in the range  $\theta \in [0, \pi]$ , and two maxima, two minima and four zeros over  $\phi$ , due to the  $\cos(2\phi)$  term in the range  $\phi \in [0, 2\pi]$ .

In this book more than one single notation is used to represent functions on the unit sphere. A common notation uses the angles of the spherical coordinate system directly, i.e.

$$f(\theta, \phi), \quad (\theta, \phi) \in S^2. \quad (1.6)$$

Sometimes a more compact notation is desired, in which case the two angles will be denoted by a single parameter, e.g.  $\mu \equiv \mu(\theta, \phi)$ , using the function representation

$$f(\mu), \quad \mu \equiv \mu(\theta, \phi) \in S^2. \quad (1.7)$$

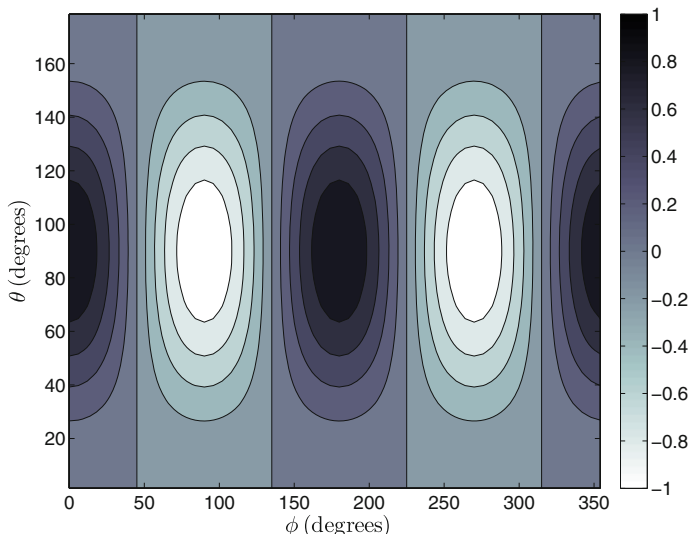


**Fig. 1.3** Plot of function  $f(\theta, \phi) = \sin^2 \theta \cos(2\phi)$  over the  $\theta\phi$  plane

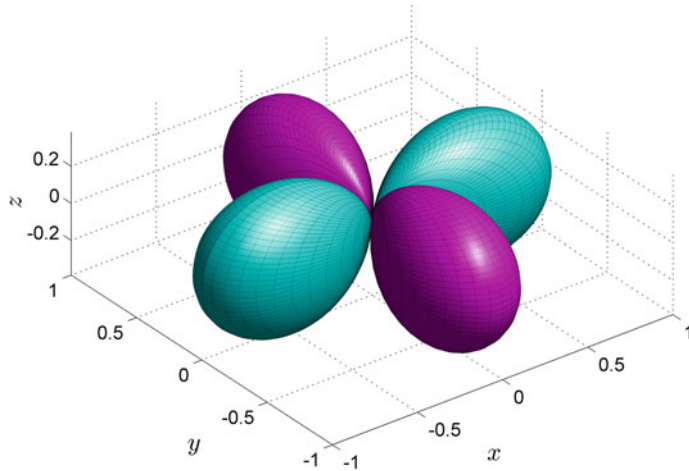


**Fig. 1.4** Balloon plot of function  $f(\theta, \phi) = \sin^2 \theta \cos(2\phi)$ , with the distance from the origin defined by  $|f(\theta, \phi)|$ , and with cyan (green-blue) shades representing positive values of  $f$ , and magenta (purple-red) shades representing negative values of  $f$

Finally, it may be desired to represent the sphere surface in Cartesian coordinates, in which case the following notation is used:

$$f(\mathbf{x}), \quad \mathbf{x} = (\sin \theta \cos \phi, \sin \theta \sin \phi, \cos \theta) \in S^2. \quad (1.8)$$

## 1.2 Spherical Harmonics

In the sections that follow, functions on the unit sphere are presented as a weighted sum of a set of basis functions, also forming the Fourier basis for functions on the sphere. These basis functions are the spherical harmonics, defined as follows [56]:

$$Y_n^m(\theta, \phi) \equiv \sqrt{\frac{2n+1}{4\pi} \frac{(n-m)!}{(n+m)!}} P_n^m(\cos \theta) e^{im\phi}, \quad (1.9)$$

where  $(\cdot)!$  represents the factorial function,  $P_n^m(\cdot)$  are the associated Legendre functions,  $m \in \mathbb{Z}$  is an integer denoting the function degree and  $n \in \mathbb{N}$  is a natural number denoting the function order.

Table 1.1 presents expressions for the spherical harmonics of orders zero to four [54]. Note that the spherical harmonics have a complex exponential dependence on  $\phi$ , so that the absolute value,  $|Y_n^m(\theta, \phi)|$ , will be constant along  $\phi$ . Therefore, plots of the real and imaginary parts of the spherical harmonics are typically presented, rather than plots of the magnitude and phase. The order  $n$  determines the highest power of

**Table 1.1** Spherical harmonics  $Y_n^m(\theta, \phi)$  for orders  $n = 0, \dots, 4$

$n = 0$	$Y_0^0(\theta, \phi) = \sqrt{\frac{1}{4\pi}}$
$n = 1$	$Y_1^{-1}(\theta, \phi) = \sqrt{\frac{3}{8\pi}} \sin \theta e^{-i\phi}$
	$Y_1^0(\theta, \phi) = \sqrt{\frac{3}{4\pi}} \cos \theta$
	$Y_1^1(\theta, \phi) = -\sqrt{\frac{3}{8\pi}} \sin \theta e^{i\phi}$
$n = 2$	$Y_2^{-2}(\theta, \phi) = \sqrt{\frac{15}{32\pi}} \sin^2 \theta e^{-2i\phi}$
	$Y_2^{-1}(\theta, \phi) = \sqrt{\frac{15}{8\pi}} \sin \theta \cos \theta e^{-i\phi}$
	$Y_2^0(\theta, \phi) = \sqrt{\frac{5}{16\pi}} (3 \cos^2 \theta - 1)$
	$Y_2^1(\theta, \phi) = -\sqrt{\frac{15}{8\pi}} \sin \theta \cos \theta e^{i\phi}$
	$Y_2^2(\theta, \phi) = \sqrt{\frac{15}{32\pi}} \sin^2 \theta e^{2i\phi}$
$n = 3$	$Y_3^{-3}(\theta, \phi) = \sqrt{\frac{35}{64\pi}} \sin^3 \theta e^{-3i\phi}$
	$Y_3^{-2}(\theta, \phi) = \sqrt{\frac{105}{32\pi}} \cos \theta \sin^2 \theta e^{-2i\phi}$
	$Y_3^{-1}(\theta, \phi) = \sqrt{\frac{21}{64\pi}} (5 \cos^2 \theta - 1) \sin \theta e^{-i\phi}$
	$Y_3^0(\theta, \phi) = \sqrt{\frac{7}{16\pi}} (5 \cos^3 \theta - 3 \cos \theta)$
	$Y_3^1(\theta, \phi) = -\sqrt{\frac{21}{64\pi}} (5 \cos^2 \theta - 1) \sin \theta e^{i\phi}$
	$Y_3^2(\theta, \phi) = \sqrt{\frac{105}{32\pi}} \cos \theta \sin^2 \theta e^{2i\phi}$
$n = 4$	$Y_4^{-4}(\theta, \phi) = \sqrt{\frac{315}{512\pi}} \sin^4 \theta e^{-4i\phi}$
	$Y_4^{-3}(\theta, \phi) = \sqrt{\frac{315}{64\pi}} \cos \theta \sin^3 \theta e^{-3i\phi}$
	$Y_4^{-2}(\theta, \phi) = \sqrt{\frac{45}{128\pi}} (7 \cos^2 \theta - 1) \sin^2 \theta e^{-2i\phi}$
	$Y_4^{-1}(\theta, \phi) = \sqrt{\frac{45}{64\pi}} (7 \cos^3 \theta - 3 \cos \theta) \sin \theta e^{-i\phi}$
	$Y_4^0(\theta, \phi) = \sqrt{\frac{9}{256\pi}} (35 \cos^4 \theta - 30 \cos^2 \theta + 3)$
	$Y_4^1(\theta, \phi) = -\sqrt{\frac{45}{64\pi}} (7 \cos^3 \theta - 3 \cos \theta) \sin \theta e^{i\phi}$
	$Y_4^2(\theta, \phi) = \sqrt{\frac{45}{128\pi}} (7 \cos^2 \theta - 1) \sin^2 \theta e^{2i\phi}$
	$Y_4^3(\theta, \phi) = -\sqrt{\frac{315}{64\pi}} \cos \theta \sin^3 \theta e^{3i\phi}$
	$Y_4^4(\theta, \phi) = \sqrt{\frac{315}{512\pi}} \sin^4 \theta e^{4i\phi}$

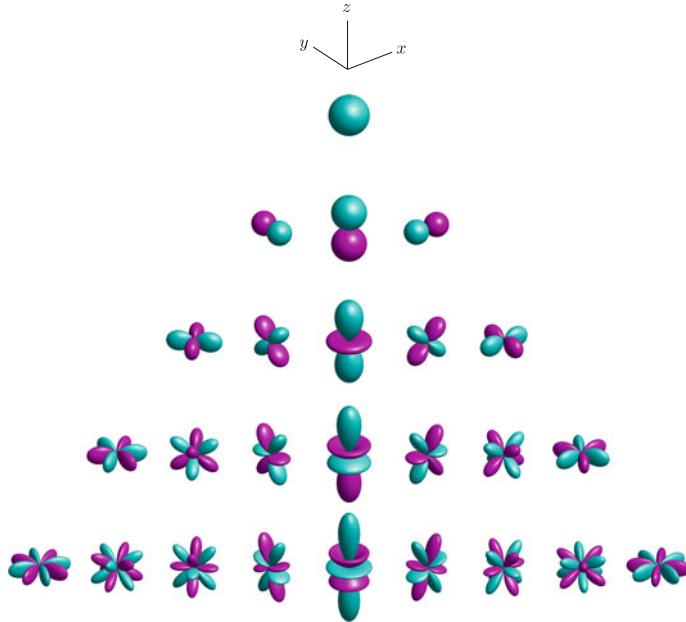


**Fig. 1.5** Balloon plot of the spherical harmonics for  $n = 0$  (top row) to  $n = 4$  (bottom row), with  $Y_n^0(\theta, \phi)$ , which is a real function, presented in the central column.  $\text{Im}\{Y_n^m(\theta, \phi)\}$  for  $-n \leq m \leq -1$  are presented in the left-hand side columns, and  $\text{Re}\{Y_n^m(\theta, \phi)\}$  for  $1 \leq m \leq n$  are presented in the right-hand side columns. The view direction is indicated by the orientation of the axes presented at the top of the figure. Colors indicate the sign of the spherical harmonic functions, with cyan (green-blue) shades representing positive values, and magenta (purple-red) shades representing negative values

the  $\cos \theta$  and  $\sin \theta$  terms controlling the dependence of the spherical harmonics over  $\theta$ , while  $m$  determines the dependence over  $\phi$  through the exponential term  $e^{im\phi}$ .

Figure 1.5 presents balloon plots of the real and imaginary parts of the spherical harmonics,  $\text{Re}\{Y_n^m(\theta, \phi)\}$  and  $\text{Im}\{Y_n^m(\theta, \phi)\}$ , with a view angle of  $(\theta, \phi) = (60^\circ, -127.5^\circ)$ . The rows in the figure present plots for  $n = 0$  (top row) to  $n = 4$  (bottom row), while the columns present plots for  $m = -n$  (leftmost column) to  $m = n$  (rightmost column).  $\text{Im}\{Y_n^m(\theta, \phi)\}$  is presented for  $m < 0$ ,  $\text{Re}\{Y_n^m(\theta, \phi)\}$  is presented for  $m > 0$ , and  $Y_n^0(\theta, \phi)$ , which is real, is presented in the central column. Table 1.2 explicitly illustrates the functions presented in Fig. 1.5, for clarity. Figure 1.5 shows that  $Y_0^0$  is constant over the sphere, similar to a monopole function. The real and imaginary parts of the spherical harmonics of order  $n = 1$  have dipole-like shapes, while higher orders have more complex forms, with the number of lobes increasing with  $n$  and  $m$ .

With the aim of visualizing the spherical harmonics more clearly, Fig. 1.6 presents the spherical harmonics in a similar manner to Fig. 1.5 but as viewed from the  $z$ -axis, i.e. downwards from above. In this case, the behavior of the real and imaginary parts

**Table 1.2** Illustration of the functions presented in Fig. 1.5

$Y_0^0$
$\text{Im} \{Y_1^{-1}\} Y_1^0 \text{Re} \{Y_1^1\}$
$\text{Im} \{Y_2^{-2}\} \text{Im} \{Y_2^{-1}\} Y_2^0 \text{Re} \{Y_2^1\} \text{Re} \{Y_2^2\}$
$\text{Im} \{Y_3^{-3}\} \text{Im} \{Y_3^{-2}\} \text{Im} \{Y_3^{-1}\} Y_3^0 \text{Re} \{Y_3^1\} \text{Re} \{Y_3^2\} \text{Re} \{Y_3^3\}$
$\text{Im} \{Y_4^{-4}\} \text{Im} \{Y_4^{-3}\} \text{Im} \{Y_4^{-2}\} \text{Im} \{Y_4^{-1}\} Y_4^0 \text{Re} \{Y_4^1\} \text{Re} \{Y_4^2\} \text{Re} \{Y_4^3\} \text{Re} \{Y_4^4\}$

of the spherical harmonics over the azimuth angle  $\phi$  is illustrated clearly. All spherical harmonics at  $m = 0$  are constant over  $\phi$ , while exhibiting  $\cos(m\phi)$  behavior for the real parts, and  $\sin(m\phi)$  behavior for the imaginary parts. The plots on the left side (imaginary part,  $m < 0$ ) are therefore rotated versions of the plots on the right side (real part,  $m > 0$ ), by  $90^\circ/m$ .

Figures 1.7 and 1.8 follow the same approach as Fig. 1.6, but with  $x$ -axis and  $y$ -axis viewpoints, respectively, showing the dependence on  $\theta$  more clearly. Spherical harmonics  $Y_n^0$  have a high value around  $\theta = 0$  and  $\theta = \pi$  due to the  $\cos^n \theta$  terms. The behavior of the other spherical harmonics is more complex. For example, spherical harmonics  $Y_n^n$  and  $Y_n^{-n}$  have a  $\sin^n \theta$  dependence, producing “flat” looking functions from the viewpoints shown in Figs. 1.7 and 1.8.

Some of the properties of the spherical harmonics are presented next, starting with basic properties and progressing to properties involving integration and summation.

- *Complex conjugate.* The spherical harmonics are complex functions due to the complex exponential term,  $e^{im\phi}$ , while the associated Legendre functions,  $P_n^m(\cos \theta)$ , are all real. The complex conjugate of the spherical harmonics take the form

$$[Y_n^m(\theta, \phi)]^* = (-1)^m Y_n^{-m}(\theta, \phi), \quad (1.10)$$

which is derived from the expression of the associated Legendre function for negative values of  $m$  [see Eq. (1.31)]. The complex conjugate property also defines the relation between  $Y_n^m(\theta, \phi)$  and  $Y_n^{-m}(\theta, \phi)$ , which are spherical harmonics of the same order and opposite degrees.

- *Limit on degree value,  $m$ .* By definition, spherical harmonics with a degree that is higher than the order are zero, i.e.

$$Y_n^m(\theta, \phi) = 0 \quad \forall |m| > n. \quad (1.11)$$

- *Zeros of the spherical harmonics.* The spherical harmonics contain  $\sin^{|m|} \theta$  terms, defining the zeros of the function for  $m \neq 0$ , i.e.

$$Y_n^m(0, \phi) = Y_n^m(\pi, \phi) = 0 \quad \forall m \neq 0. \quad (1.12)$$

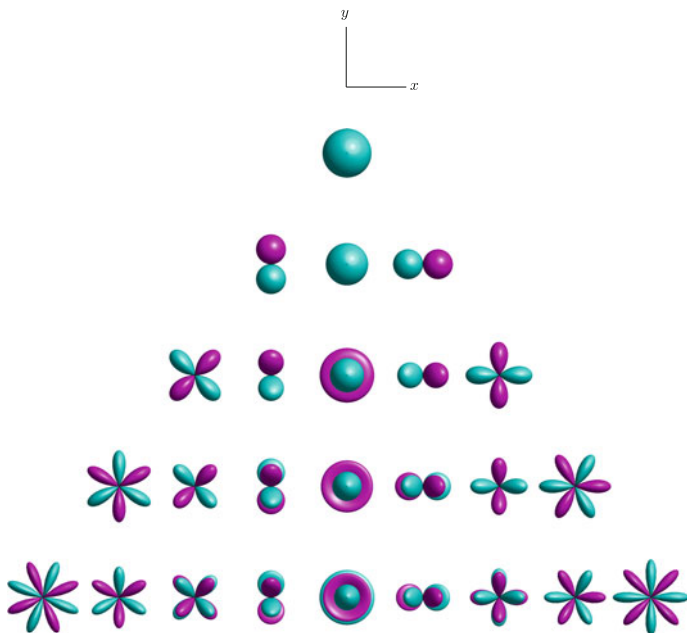


**Fig. 1.6** Same as Fig. 1.5, but viewed from the  $z$ -axis (*top view*)

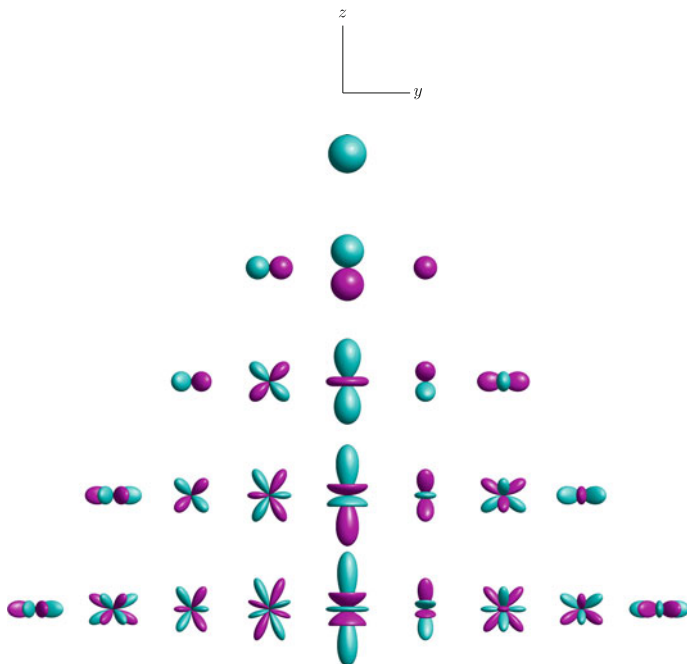


**Fig. 1.7** Same as Fig. 1.5, but viewed from the  $x$ -axis (*front view*)

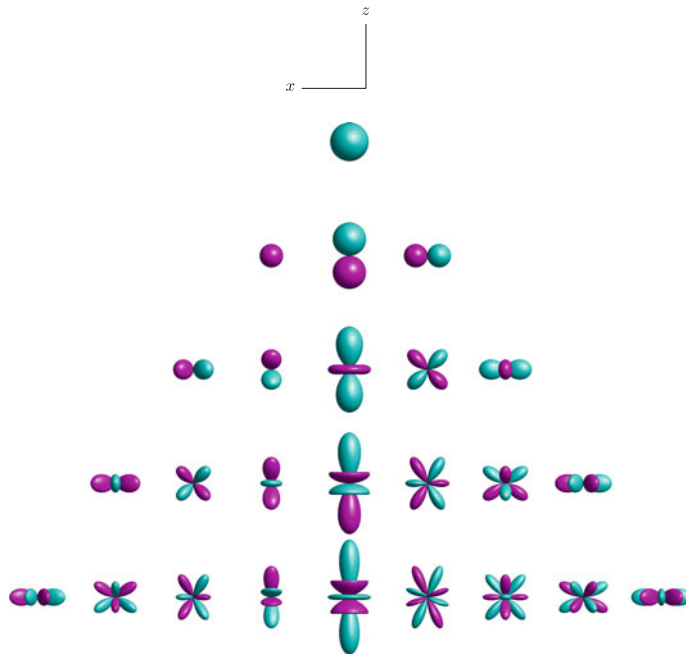


**Fig. 1.8** Same as Fig. 1.5, but viewed from the  $y$ -axis (*side view*)

- *Spherical harmonics at  $m = 0$ .* At  $m = 0$ , the associated Legendre function degenerates to the Legendre polynomials (see Sect. 1.3) and so the spherical harmonics have a simplified expression:

$$Y_n^0(\theta, \phi) = \sqrt{\frac{2n+1}{4\pi}} P_n(\cos \theta). \quad (1.13)$$

These spherical harmonics are not dependent on  $\phi$  and are therefore axis-symmetric relative to the  $z$ -axis. This is clearly illustrated in Figs. 1.7 and 1.8, by the spherical harmonic functions on the central columns.

- *Spherical harmonics at  $m = n$  and  $m = -n$ .* At these extreme values of  $m$ , the spherical harmonics have a sine dependence on  $\theta$  and a simplified form:

$$\begin{aligned} Y_n^{-n}(\theta, \phi) &= \frac{1}{2^{n+1} n!} \sqrt{\frac{(2n+1)!}{\pi}} \sin^n \theta e^{-in\phi} \\ Y_n^n(\theta, \phi) &= \frac{(-1)^n}{2^{n+1} n!} \sqrt{\frac{(2n+1)!}{\pi}} \sin^n \theta e^{in\phi}. \end{aligned} \quad (1.14)$$

- *Mirror symmetry along  $\theta$  with respect to the equator,  $\theta = \pi/2$ .* The spherical harmonics have a mirror symmetry in  $\theta$ , such that the function on the upper hemisphere is equal to the function on the lower hemisphere, up to a sign factor:

$$Y_n^m(\pi - \theta, \phi) = (-1)^{n+m} Y_n^m(\theta, \phi). \quad (1.15)$$

This symmetry is clearly illustrated in Figs. 1.7 and 1.8 by the real and imaginary parts of the spherical harmonics, in which the sign is indicated by color. For even  $n + m$  the functions are symmetric about the equator, whereas for odd  $n + m$  the functions are antisymmetric about the equator.

- *Symmetry with respect to  $\phi$ .* The spherical harmonics have mirror symmetry with respect to  $\phi$  due to the exponential function, such that

$$Y_n^m(\theta, \phi + \pi) = (-1)^m Y_n^m(\theta, \phi). \quad (1.16)$$

This property is illustrated in Fig. 1.6, where spherical harmonic functions for even values of  $m$  are equal at opposite sides of the circle defined by  $\phi$ , while for odd values of  $m$  the functions have the opposite sign (different color) at a phase shift of  $180^\circ$  along  $\phi$ .

Another symmetry along  $\phi$  is defined relative to the  $x$ -axis, again due to the behavior of the exponential function:

$$Y_n^m(\theta, -\phi) = [Y_n^m(\theta, \phi)]^*. \quad (1.17)$$

Figure 1.6 illustrates that the real part of the spherical harmonics, plotted on the right-hand side columns, is symmetric about the  $x$ -axis, while the imaginary part is antisymmetric.

- *Opposite direction.* Combining the last two properties, Eqs. (1.15) and (1.16), the spherical harmonics at  $(\pi - \theta, \phi + \pi)$ , which is the opposite direction to  $(\theta, \phi)$ , can be written as

$$Y_n^m(\pi - \theta, \phi + \pi) = (-1)^n Y_n^m(\theta, \phi). \quad (1.18)$$

- *Periodicity with respect to  $\phi$ .* The spherical harmonics are periodic with respect to  $\phi$  with a period of  $2\pi/m$ , due to the exponential term  $e^{im\phi}$ , and therefore satisfy

$$Y_n^m(\theta, \phi + 2\pi/m) = Y_n^m(\theta, \phi). \quad (1.19)$$

The periodicity is illustrated in Fig. 1.6, where, for example, the spherical harmonics on the central column with  $m = 0$  are constant along  $\phi$ , spherical harmonics corresponding to  $m = \pm 1$  have a period of  $2\pi$ , those corresponding to  $m = \pm 2$  have a period of  $\pi$ , and so on.

The next set of properties is related to the integration of the spherical harmonic functions over the unit sphere. In general, integration over a sphere of radius  $r$  can be calculated by dividing the sphere area into elements, as illustrated in Fig. 1.9. The length along  $\phi$  of each element on the sphere surface is given by  $r \sin \theta d\phi$ , denoting the fact that the elements are narrower in the azimuth dimension nearer the poles. The width along  $\theta$  of each element is given by  $rd\theta$ . The area element is therefore defined as

$$r^2 d\Omega = r^2 \sin \theta d\theta d\phi, \quad (1.20)$$